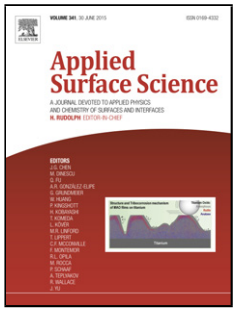


Title: Self-organized nano-structuring of CoO islands on Fe(001)

Author: A. Brambilla A. Picone D. Giannotti M. Riva G. Bussetti G. Berti A. Calloni M. Finazzi F. Ciccacci L. Duò

PII: S0169-4332(15)02924-4
DOI: http://dx.doi.org/doi:10.1016/j.apsusc.2015.11.217
Reference: APSUSC 31935

To appear in: *APSUSC*

Received date: 6-11-2015
Accepted date: 22-11-2015

Please cite this article as: A. Brambilla, A. Picone, D. Giannotti, M. Riva, G. Bussetti, G. Berti, A. Calloni, M. Finazzi, F. Ciccacci, L. Du*graveo*, Self-organized nano-structuring of CoO islands on Fe(001), *Applied Surface Science* (2015), http://dx.doi.org/10.1016/j.apsusc.2015.11.217

CoO grown on the Co(001)-*p*(1×1)O surface of a 5 ML thick Co layer on Fe(001)

The growth process does not induce Fe cation migration and/or oxidation

A misfit dislocation network develops in the very early stages of CoO growth.

Such a network acts as a template for a three-dimensional CoO nanostructuration

The dimensions of CoO wedding-cake square mounds scale linearly with thickness

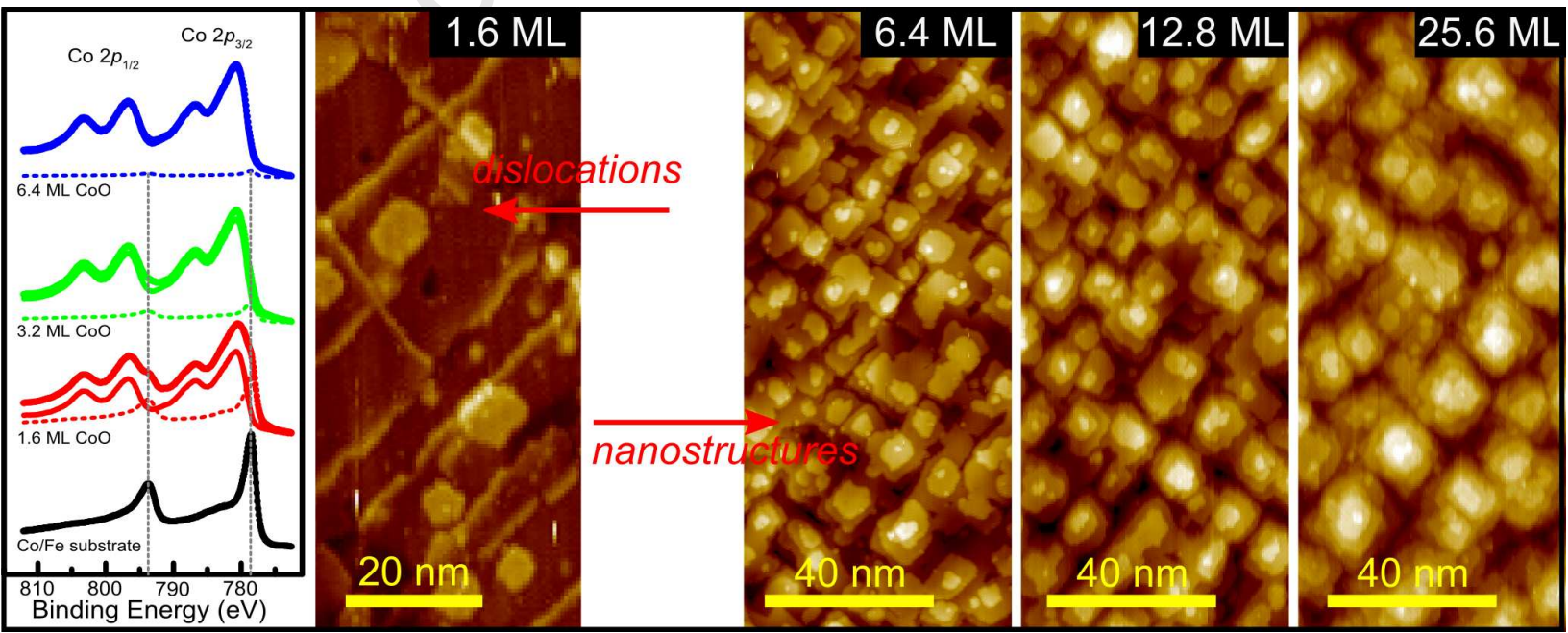

# Self-organized nano-structuring of CoO islands on Fe(001)

A. Brambilla[a,*], A. Picone[a], D. Giannotti[a], M. Riva[a,1], G. Bussetti[a], G. Berti[a], A. Calloni[a], M. Finazzi[a], F. Ciccacci[a], L. Duò[a]

[a] *Politecnico di Milano, piazza Leonardo da Vinci, 32 - 20133 Milano (Italy)*

## Abstract

The realization of nanometer-scale structures through bottom-up strategies can be accomplished by exploiting a buried network of dislocations. We show that, by following appropriate growth steps in ultra-high vacuum molecular beam epitaxy, it is possible to grow nano-structured films of CoO coupled to Fe(001) substrates, with tunable sizes (both the lateral size and the maximum height scale linearly with coverage). The growth mode is discussed in terms of the evolution of surface morphology and chemical interactions as a function of the CoO thickness. Scanning tunneling microscopy measurements reveal that square mounds of CoO with lateral dimensions of less than 25 nm and heights below ten atomic layers are obtained by growing few-nanometers-thick CoO films on a pre-oxidized Fe(001) surface covered by an ultra-thin Co buffer layer. In the early stages of growth, a network of misfit dislocations develops, which works as a template for the CoO nano-structuring. From a chemical point of view, at variance with typical CoO/Fe interfaces, neither Fe segregation at the surface nor Fe oxidation at the buried interface are observed, as seen by Auger electron spectroscopy and X-ray Photoemission Spectroscopy, respectively.

*Keywords:*
cobalt oxide, iron, self-organization, electron spectroscopies, scanning tunneling microscopy

*Corresponding author
*Email address:* alberto.brambilla@polimi.it (A. Brambilla)
[1]Current address: Institute of Applied Physics, TU-Wien, Wiedner Hauptstraße 8-10, 1040 Vienna (Austria)

## 1. Introduction

There is nowadays a constantly growing interest towards the study of nanostructured materials. Among different possible fabrication approaches, those classified as bottom-up, which consist in exploiting the peculiarity of the growth procedure in order to obtain self-organized systems at the nanometer scale, combine both fundamental and technological potentialities [1, 2]. The former is due to the fact that many materials, when confined to low dimensions, show novel and intriguing properties. The latter stems from the paramount importance of miniaturization for many devices, from electronics, to magnetism, to catalytic applications, only to mention a few general cases.

In this scenario, a known route to realize ordered nanostructures through self-organization consists in exploiting the development of ordered networks of defects in epitaxial layered structures [3]. Such a strategy has already been successful in many cases where, in particular, either metallic or semiconducting ordered nano-structure assemblies have been obtained by growing the relative materials on interfaces containing dislocation networks [3–6]. In other cases, the growth of nanostructures has been realized on oxide substrates similarly characterized by a peculiar distribution of defects [7–9]. Much scarcer appears to be the record of cases in which the nanostructured systems consist of the oxide materials themselves [10, 11].

In this paper, we report on the observation of nanostructured cobalt oxide (CoO) films with tunable sizes, grown on top of oxygen-passivated Co ultra-thin films on Fe(001). CoO is a compound of very broad interest in particular in the fields of catalysis [12, 13], energy storage [14–16] and magnetism [17–24], being an antiferromagnetic insulator. Furthermore, CoO films coupled to ferromagnetic substrates (like Fe), show the well-known and technologically important exchange bias effect [25, 26], which makes this kind of systems even more appealing. Previous investigations on CoO/Fe(001) layered structures reported on complicated and extended chemical reactions at the interface, which is common when transition metal oxides are grown on the reactive Fe substrate [18, 27–29]. Scanning Tunneling Microscopy (STM) measurements observed a three-dimensional growth of CoO without any particular order [30]. In the present case, we have grown CoO by reactive deposition on Fe(001) substrates covered by a ultra-thin buffer layer of metallic Co. This approach leads to a substantial reduction of the chemical mixing at the interface and, at the same time, induces the development of a network of

misfit dislocations over which well-ordered wedding cake CoO islands begin to form after a few atomic layers. Such islands have a square shape, with edges parallel to the equivalent $< 100 >$ in-plane directions of the cubic CoO crystal structure. Their lateral size increases with coverage, up to about 25 nm for a nominal CoO thickness of about 7 nm, keeping a noticeable spatial regularity.

## 2. Experimental methods

The samples were fabricated by growing a 500 nm thick Fe film onto a Ultra-High Vacuum (UHV)-cleaned MgO(001) crystal substrate, by means of molecular beam epitaxy (MBE) performed at room temperature (RT). The Fe(001) surface was then exposed to 30 L (1 L = $1.33 \times 10^{-4}$ Pa·s) of molecular oxygen right after being annealed at 700 K and finally it was flash heated at 900 K. This recipe allowed us to obtain the well-characterized Fe(001)-$p(1 \times 1)$O surface, in which each surface unit cell has one oxygen atom in the fourfold symmetrical Fe hollow site [31, 32]. A 5 monolayers (ML) thick buffer layer of metallic Co was grown onto the Fe(001)-$p(1 \times 1)$O surface. In such a thickness range, Co is known to grow pseudomorphically on the Fe substrate [33, 34], with a body centered tetragonal (bct) structure and the same in-plane lattice parameter as bulk Fe ($a_{\mathrm{Fe}} = 0.287$ nm). The growth of thin Co films on Fe(001)-$p(1 \times 1)$O is known to proceed in a layer-by-layer (also known as Frank-van der Merwe) mode, as demonstrated by former studies [33, 35] and confirmed by our STM observations [36]. The Co growth was performed at RT by means of MBE through an e-beam evaporator in UHV (base pressure in the $10^{-9}$ Pa range), then the sample was heated at 470 K for about 5 minutes. As in other similar cases [32, 37–40], the oxygen segregates to the sample surface and this procedure results in a Co(001)-$p(1 \times 1)$O surface, as testified by Low-Energy Electron Diffraction (LEED) and STM [36]. Cobalt oxide is then grown at 470 K by reactive deposition of metallic Co in a pure $O_2$ atmosphere, with partial pressure $p_{O_2} = 1 \cdot 10^{-4}$ Pa, with thicknesses up to about 32 ML (1 ML of CoO is nominally equal to 0.213 nm). Bulk CoO has a fcc structure with lattice parameter $a_{\mathrm{CoO}} = 0.426$ nm and the surface atomic arrangement of the Co layer is the same as for Fe(001). In this way, the oxide can epitaxially grow by exposing the (001) surface, with the cubic cell rotated by 45° with respect to the substrate, i.e. with the $< 100 >$ in-plane directions parallel to the $< 110 >$ in-plane directions of Fe.

STM images were acquired by an Omicron VT instrument in a UHV chamber (base pressure $10^{-9}$ Pa) directly connected to the preparation system. STM measurements were performed in constant-current mode with home-made electrochemically etched W tips. The chemistry of the growing CoO/Co/Fe samples was investigated *in situ* by means of Auger Electron Spectroscopy (AES). The AES measurements were performed by means of an Omicron SPECTALEED with a retarding field analyzer (total acceptance angle 102°), operated with a 3 kV, 20 $\mu$A primary electron beam, with a 3 V peak-to-peak modulation amplitude. The same instrument was used in order to record LEED patterns. Moreover, X-ray Photoemission Spectroscopy (XPS) was performed in order to further study the chemistry of the buried interface. The XPS spectra were acquired by exploiting a Mg source ($h\nu$ = 1253.6 eV) and a Phoibos 150 hemispherical analyzer (both instruments are from Specs GmbH) in a separated UHV chamber in which the samples were freshly prepared on purpose. All of the above measurements were performed at RT.

## 3. Results and discussion

Low-energy Auger peaks in AES spectra, corresponding to Fe and Co MNN transitions, are known to be extremely sensitive to the local chemical environment of the atoms (see, for instance, Refs. 39, 41 for Fe oxidation and Refs. 42, 43 for Co oxidation). Fig. 1 reports a series of AES spectra of the investigated samples, where the relevant features are marked by vertical lines. In particular, these are related to metallic Fe (46.8 eV), metallic Co (52.5 eV), oxidized Fe (39.0 eV and 49.7 eV) and oxidized Co (37.0 eV and 43.7 eV). The series starts from the Co(001)-$p(1\times1)$O surface of a 5 ML thick Co layer grown onto Fe(001)-$p(1\times1)$O (indicated as Co/Fe substrate) and passes through the early stages of CoO growth (up to 6.4 CoO ML). Along such profiles, the valley feature related to metallic Co is clearly reduced upon CoO thickening, while the peak related to oxidized Co correspondingly increases, as expected. For higher CoO thicknesses, the low-energy Auger spectra are substantially unchanged, keeping a CoO-like line shape in good agreement with previous investigations [42, 43].

Substantially, no traces of Fe oxides are seen in these spectra, as confirmed by comparing them to a spectrum acquired from a bare Fe(001) film oxidized by exposure to 50 L of molecular oxygen, which is reported as a dotted line in Fig. 1. Also, no further traces of a metallic Fe signal can be seen, after the

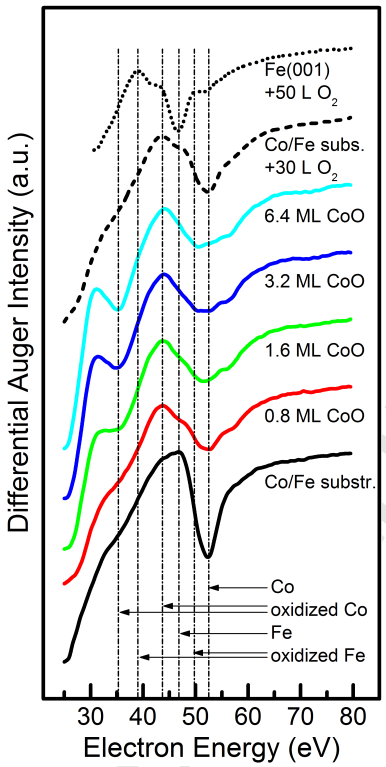


Figure 1: AES spectra related to Fe and Co MNN transitions, as a function of the CoO coverage. Co/Fe substrate refers to the Co(001)-$p(1 \times 1)$O surface of a 5 ML thick Co layer on Fe(001). The topmost spectra are shown for comparison and refer to a Fe(001) sample exposed to 50 L of oxygen (dotted line) and to the Co/Fe substrate exposed to 30 L of oxygen (dashed line), respectively. The positions of characteristic Fe and Co features (either peaks or valleys) are highlighted by vertical lines.

shoulder visible in the Co/Fe substrate spectra is attenuated by the growing CoO film. These observations indicate that the CoO film grows onto the Co/Fe substrate without inducing significant Fe segregation (and subsequent oxidation), at variance with the case of reactive deposition of CoO directly onto the Fe(001)-$p(1 \times 1)$O surface [28]. This result is quite surprising, since the standard enthalpy of formation of CoO is higher ($\Delta_f H^0$ = -238 kJ/ mol O) than that of Fe oxides ($\Delta_f H^0$ = -272 kJ/ mol O for FeO, which has the higher value), resulting in a lower oxygen affinity for Co than for Fe [44]. Indeed, Fe segregation has been observed in the post-oxidation of ultra-thin Ni (that, as Co, has a lower oxygen affinity than Fe) films on Fe(001) [41, 45]. The absence of Fe segregation is further confirmed by inspecting the

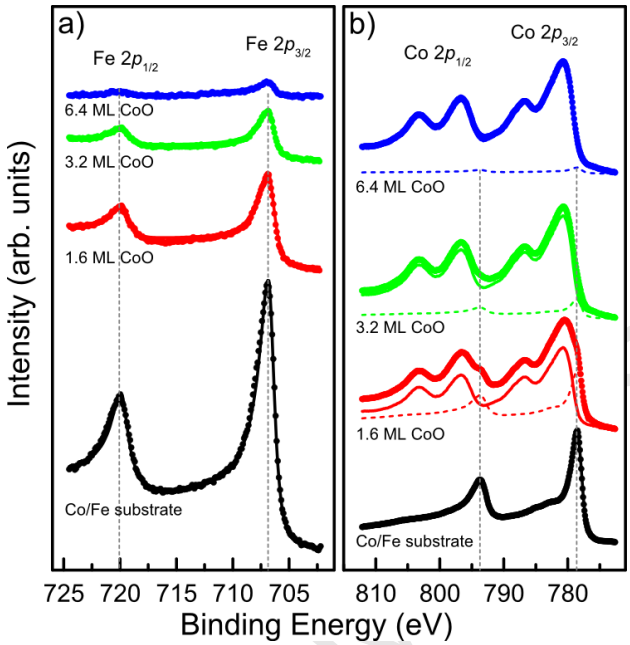


Figure 2: Normal emission XPS spectra related to: a) the Fe 2*p* energy region (circles are the raw data, continuous lines are the fittings); b) the Co 2*p* energy region (circles are the raw data, continuous lines are the fittings of the oxidized components; dashed lines are the fittings of the metallic components). From bottom to top, the spectra are reported as a function of the CoO coverage. Co/Fe substrate refers to the Co(001)-$p(1 \times 1)$O surface of a 5 ML thick Co layer on Fe(001).

low-energy AES spectrum of the Co/Fe substrate after exposing it to 30 L of molecular oxygen, which is reported as a dashed line in Fig. 1. Here, again, no traces of either metallic or oxidized Fe can in fact be detected.

Further pieces of information about the chemistry of the buried interface can be obtained by the XPS spectra reported in Fig. 2. Compared to AES experiments, the XPS measurements are characterized by a larger escape depth, on account of the larger kinetic energy of the emitted electrons. In particular, for the present case, current models for the calculation of the electron inelastic mean free path predict that the latter is as low as 0.4 nm at a kinetic energy of 50 eV (AES case), to be compared to about 1.1 nm at a kinetic energy of about 450-550 eV (XPS case) [46]. XPS is therefore more suited to analyze the buried interface.

Fig. 2a) shows the Fe 2*p* energy region, for the Co/Fe substrate (5 ML Co, as above) and ultra-thin CoO films of 1.6 ML, 3.2 ML and 6.4 ML. The

measured spectra are represented by circles, while continuous lines are sums of fittings made up of typical line shapes. The Fe $2p$ spectrum can, in particular, be fitted by line shapes mimicking the Doniach-Sunjic asymmetric line shape, which is typical of metallic materials, without the need to introduce any additional peak possibly related with the presence of oxides. This agrees well with the fact that, upon Co deposition, oxygen floats to the topmost Co layers and leaves metallic Fe at the interface. At higher CoO coverages the corresponding Fe $2p$ spectra keep their metallic character, while decreasing in intensity due to the electron attenuation from the overlayer.

Fig. 2b) shows the Co $2p$ energy region. Here, the first significant information is the line shape of the 6.4 ML thick CoO layer (top spectrum), which agrees very well with that expected for a CoO film [28, 43, 47, 48]. Such a line shape did not change at higher thicknesses (not shown). On the other hand, the spectrum of the Co/Fe substrate has a clear metallic character, similarly to the Fe $2p$ case. A small shoulder next to the Co $2p_{3/2}$ peak (at higher binding energy) is consistent with the presence of one layer of oxygen at the vacuum interface [49]. Concerning the CoO layers of intermediate thicknesses (1.6 ML and 3.2 ML), the line shapes can be correctly fitted only by considering the presence of both oxidized (continuous lines) and metallic (dashed lines) features. Only a tiny metallic component can be derived for the 6.4 ML spectrum. Given the low thickness of the CoO film compared to the estimated electron escape depth (see above), as testified by the fact that the signal from the Fe $2p$ region is still visible at a 6.4 ML nominal coverage, we conclude that the Co buffer layer gets oxidized while the CoO film is grown by reactive deposition. Moreover, the metallic character of the the Fe $2p$ spectra allows us to conclude that such an oxidation did not extend to the Co/Fe interface, thus leaving a thin Co metallic buffer layer whose thickness can be varied by appropriately selecting the growth conditions and the thickness of the initial bct Co layer. In particular, the thickness of such a buffer layer can be comprised in a relatively wide range from about 3 to 17 atomic layers, where the growth of bct Co onto Fe(001)-$p(1 \times 1)$O proceeds in a nearly perfect layer-by-layer mode [36].

Coming to the morphology of the growing CoO/Co/Fe(001) layered structure, at sub-monolayer coverages the growing oxide wets the Co(001)-$p(1 \times 1)$O surface, without presenting any particular feature (not shown). Slightly above 1 ML, a series of ordered bright rows are observed on the surface, as in Fig 3a) for a 1.6 ML coverage. They are clearly oriented along the in-plane $< 110 >$ directions of Fe, which correspond to the in-plane $< 100 >$

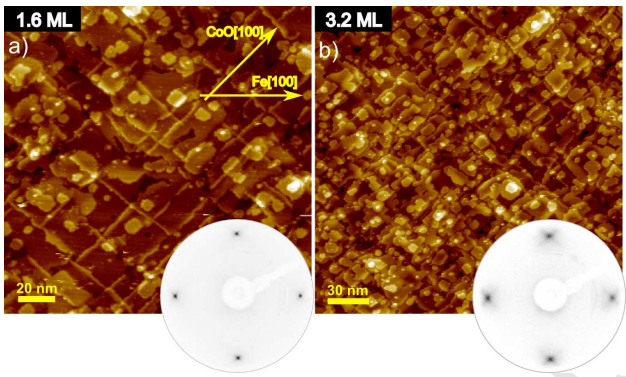


Figure 3: STM images of: a) 1.6 ML CoO ($V = -3.1$ V; $I = 1$ pA) and b) 3.2 ML CoO ($V = -3$ V; $I = 5$ pA) films. The insets show the LEED patterns of the corresponding surfaces, both obtained with an electron beam energy of 50 eV.

directions of the developing CoO film.

Such step-like features are the fingerprint of the presence of a square network of misfit dislocations, which is a well-known mechanism for relieving stress and strain in thin films. It has, in fact, already been observed by STM in oxide thin films such as, e.g., MgO/Fe(001) [11] and MgO/Mo(001) [50–52]. The need for the development of a misfit dislocation network can be understood on account of the mismatch between the CoO and Fe lattice constants, which corresponds to 4.9 % in the present case (CoO is subject to a compressive strain). In particular, making reference to the coincidence-site lattice model [10, 11, 36], one would expect an average dislocation periodicity of about $a_{\mathrm{CoO,P}} \cdot a_{\mathrm{Fe}}/\sqrt{2}|a_{\mathrm{CoO,P}} - a_{\mathrm{Fe}}| = 4.4$ nm. Here, $a_{\mathrm{CoO,P}} = 0.301$ nm is the lattice parameter of the primitive cell, and the minimum possible coincidence site is on the bridge epitaxial sites, rotated by 45° with respect to the primitive lattices, see Ref. 36. The presence of different spacings, typically comprised between some 5 nm and 20 nm, among the bright lines in Fig. 3a), suggests that the elastic strain was not completely released trough dislocations at this growth stage.

When the CoO thickness is increased to 3.2 ML (Fig. 3b), the growth mode clearly switches to three-dimensional island nucleation, with the formation of square mounds, whose edges appear to be aligned along the in-plane $< 100 >$ directions of CoO. All mounds are composed by monolayer steps and the surface exposes up to four layers overall (i.e. each mound is composed by a maximum of four steps).

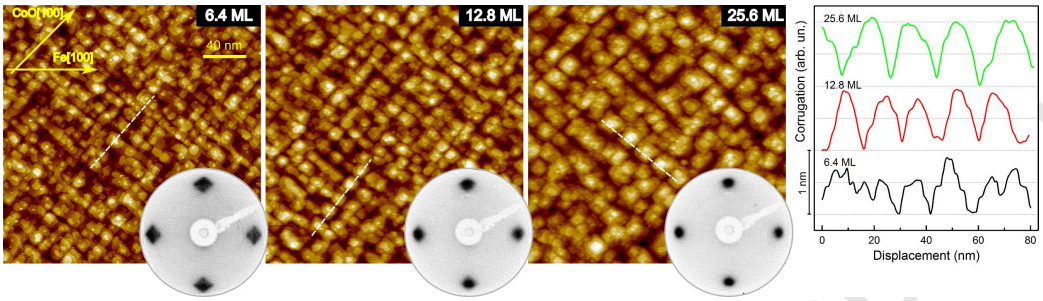


Figure 4: Left side: STM images of, from left to right, 6.4 ML CoO ($V = -3$ V; $I = 10$ pA), 12.8 ML CoO ($V = -3.1$ V; $I = 200$ pA) and 25.6 ML CoO ($V = -5$ V; $I = 100$ pA) films. All images are $200 \times 200$ nm$^2$ wide. The insets report the LEED patterns of each corresponding surface, all obtained with a electron beam energy of 50 eV. Right side: line profiles collected along the dashed lines of the corresponding STM images.

The presence of the dislocation network induces spatially periodic deformations that are visible in the LEED patterns of the sample surfaces in terms of satellite spots, which are broadened into crosses oriented along the in-plane $< 100 >$ directions of CoO. Such crosses are only weakly visible at 1.6 ML coverage (inset of Fig. 3a) and become more evident at 3.2 ML (inset of Fig. 3b). Similar effects have been reported in several other cases, related to oxide films characterized by the development of a misfit dislocation network, and were attributed to the surface mosaic spread (i.e. to the local tilting of the surface) [10, 11, 50, 51, 53, 54].

As anticipated above, the significant role of the interface dislocations is better evidenced at higher CoO thicknesses, in terms of stabilization of well-ordered CoO mounds with square bases and mesa morphology, as reported in Fig. 4. The mounds, already present for a CoO coverage of 3.2 ML, become much more uniformly distributed at 6.4 ML. Furthermore they are well separated by deep grooves. The presence of such grooves puts in evidence how the mound edges are always clearly oriented along the equivalent $< 100 >$ directions of CoO, as for the step-like features related to the misfit dislocations network. Even if no plastic deformation related to the misfit dislocation network can be clearly evidenced by STM here, the related LEED pattern (see the inset of Fig. 4, 6.4 ML CoO) is characterized by large square spots, arranged with a (1×1) symmetry with respect to the substrate. The square spots have edges oriented along the $< 100 >$ directions of CoO, most likely on account of an additional mosaic effect due to a twisting of the CoO islands, as described in details in Refs. 11 and 53.

The CoO surface morphology appears to be characterized by a visible spatial regularity also at higher thicknesses, as testified by the STM images of 12.8 ML and 25.6 ML CoO films, also reported in Fig. 4. At the same time, the dimensions of the square mounds increase linearly with increasing CoO thickness, as shown also by drawing typical line profiles along one of the in-plane $< 100 >$ directions of CoO, reported in the right panel of Fig. 4. In this scenario, it is evident that the interplay between chemistry and morphology plays a fundamental role. In particular, previous works have been evidencing that oxidation induces a strong roughening of the surface of Fe substrates [11], thus preventing the formation of coherent interfaces with oxide overlayers.

The insets of Fig. 4 show the LEED patterns of the corresponding surfaces. The rotated square spots related to the 6.4 ML thick CoO films, already discussed above, leaves gradually the place to rounded spots, more and more similar to LEED patterns of CoO thin films grown on Fe(001) without a Co buffer layer [30]. Such an evolution indicates that the degree of mosaicity of the film tend to decrease continuously with increasing thickness [50], suggesting that the plastic deformations of the oxide layer have eventually relaxed.

The switching of the sample growth mode to three-dimensional indicates that the atomic diffusion between contiguous layers (interlayer transport) has become less favorable. The limit of zero interlayer transport would correspond to a pure statistical growth, equivalent to random deposition, where vertical and lateral diffusions are substantially inhibited. This is clearly not the case here, since the morphology of the growing film is regular on a characteristic length scale (see below). The growth mode shows instead many similarities with the wedding cake model [55], in particular concerning the fact that the spatial distribution of the mounds is substantially determined by the positions of the islands nucleated on the first layer [55, 56]. In this case, they are those formed after the development of the misfit dislocation network.

The increasing size of the mounds was evaluated by generating the two-dimensional autocorrelation functions (2D-ACF) of the STM images and by measuring the first-neighbors peak distances (such an analysis was performed with the help of the WSxM software [57]). This method is exemplified in Fig. 5a), which shows some line profiles derived from the 2D-ACF calculated on STM images of the 6.4 ML, 12.8 ML and 25.6 ML CoO, respectively. Such profiles are drawn along one of the in-plane $< 100 >$ directions of CoO, as shown in the inset of Fig. 5a) for the 6.4 ML CoO case. The results reported

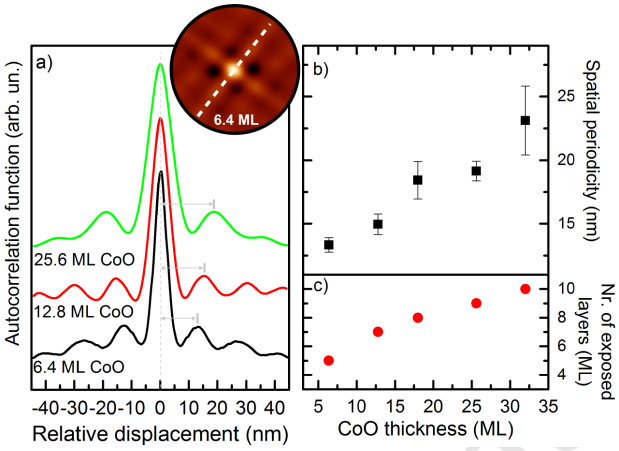


Figure 5: a) Autocorrelation functions profiles for 6.4 ML, 12.8 ML and 25.6 ML CoO thicknesses. The gray arrows show how the first-neighbors peak distances are calculated. Inset: plot of the two-dimensional autocorrelation function for 6.4 ML CoO. More bright indicates higher value. The dashed line is related to the 6.4 ML CoO autocorrelation function profile. b) Spatial periodicity of the mounds displacement as a function of the CoO coverage. c) Number of CoO layers exposed in the STM images as a function of the CoO coverage.

in Fig. 5b) show the spatial periodicity of the square mounds, which are calculated as the mean distance between the central spot and one of the first-neighbor peaks of the 2D-ACF, averaged over several STM images. Such a periodicity substantially corresponds to the lateral dimensions of the mounds, which are seen to increase from about 13 nm at 6.4 ML CoO thickness to about 23 nm for 32 ML CoO.

One difference with respect to the expectations of a wedding cake model is the fact that here we observe a partial coalescence of the mounds during growth, which is absent in the reference example of the model, namely Pt homoepitaxy on Pt(111) [55, 58]. This means that, for an ideal wedding cake growth, the spacing between mounds (and therefore their lateral dimensions) is determined by the size distribution of the first layer islands. In the present case, instead, the lateral size of the lower exposed layer increases as well. This is also testified by measuring the number of exposed layers (by using the flooding analysis function of the WSxM software [57]), which is reported in Fig. 5c). Indeed, while at 6.4 ML the number of exposed layers is similar to the nominal thickness, such a number raises, almost linearly, up to only 10 layers when the nominal CoO thickness is above 30 ML.

## 4. Conclusions

In conclusion, when CoO is grown at 470 K by reactive deposition on the Co(001)-$p(1 \times 1)$O surface of a 5 ML thick Co layer grown onto Fe(001), the growth proceeds without inducing Fe cation migration and oxidation, at variance with the growth of CoO directly on Fe(001). In such conditions, furthermore, a misfit dislocation network develops in the very early stages of CoO growth. Such a network acts as a template for a three-dimensional growth characterized by square wedding cake mounds that are regularly distributed on the surface, with sides parallel to the sides of the cubic CoO crystal structure. Both lateral size and height of such mounds scale linearly with the CoO thickness, making them tunable as a function of such a parameter alone.

This particular combination of wedding cake growth and spatial regularity is rather unique for ultra-thin oxide systems. Given the relevance that can be attributed to the self-organized growth of oxides, our system will offer an interesting workbench for testing nano-oxides growth theories.

## Acknowledgements

This work was partially supported by the Italian Ministry of University and Research through the FIRB Project nr. RBAP115AYN and by Fondazione Cariplo through the project SHAPES (grant nr. 2013-0736).

## References

[1] J. V. Barth, G. Costantini, K. Kern, Engineering atomic and molecular nanostructures at surfaces., Nature 437 (2005) 671–679.

[2] M. Einax, W. Dieterich, P. Maass, *Colloquium* : Cluster growth on surfaces: Densities, size distributions, and morphologies, Rev. Mod. Phys. 85 (2013) 921–939.

[3] H. Brune, M. Giovannini, K. Bromann, K. Kern, Self-organized growth of nanostructure arrays on strain-relief patterns, Nature 394 (1998) 451–453.

[4] F. Leroy, G. Renaud, A. Letoublon, R. Lazzari, C. Mottet, J. Goniakowski, Self-Organized Growth of Nanoparticles on a Surface Patterned by a Buried Dislocation Network, Phys. Rev. Lett. 95 (2005) 185501.

[5] B. Voigtländer, N. Theuerkauf, Ordered growth of Ge islands above a misfit dislocation network in a Ge layer on Si ( 111 ), Surf. Sci. 461 (2000) L575–L580.

[6] J. Stangl, V. Holý, G. Bauer, Structural properties of self-organized semiconductor nanostructures, Rev. Mod. Phys. 76 (2004) 725–783.

[7] P. Torelli, E. Soares, G. Renaud, L. Gragnaniello, S. Valeri, X. Guo, P. Luches, Self-organized growth of Ni nanoparticles on a cobalt-oxide thin film induced by a buried misfit dislocation network, Phys. Rev. B 77 (2008) 081409.

[8] L. Gragnaniello, T. Ma, G. Barcaro, L. Sementa, F. R. Negreiros, A. Fortunelli, S. Surnev, F. P. Netzer, Ordered Arrays of Size-Selected Oxide Nanoparticles, Phys. Rev. Lett. 108 (2012) 195507.

[9] S. Benedetti, F. Stavale, S. Valeri, C. Noguera, H. J. Freund, J. Goniakowski, N. Nilius, Steering the growth of metal ad-particles via interface interactions between a MgO thin film and a Mo support, Adv. Funct. Mater. 23 (2013) 75–80.

[10] P. Torelli, E. Soares, G. Renaud, S. Valeri, X. Guo, P. Luches, Nanostructuration of CoO film by misfit dislocations, Surf. Sci. 601 (2007) 2651–2655.

[11] A. Tekiel, S. Fostner, J. Topple, Y. Miyahara, P. Grütter, Reactive growth of MgO overlayers on Fe(001) surfaces studied by low-energy electron diffraction and atomic force microscopy, Appl. Surf. Sci. 273 (2013) 247–252.

[12] L. Liao, Q. Zhang, Z. Su, Z. Zhao, Y. Wang, Y. Li, X. Lu, D. Wei, G. Feng, Q. Yu, X. Cai, J. Zhao, Z. Ren, H. Fang, F. Robles-Hernandez, S. Baldelli, J. Bao, Efficient solar water-splitting using a nanocrystalline CoO photocatalyst., Nat. Nanotechnol. 9 (2014) 69–73.

[13] Y. Liang, H. Wang, P. Diao, W. Chang, G. Hong, Y. Li, M. Gong, L. Xie, J. Zhou, J. Wang, T. Z. Regier, F. Wei, H. Dai, Oxygen Reduction Electrocatalyst Based on Strongly Coupled Cobalt Oxide Nanocrystals and Carbon Nanotubes, J. Am. Chem. Soc. 134 (2012) 15849–15857.

[14] W. Deng, W. Lan, Y. Sun, Q. Su, E. Xie, Porous CoO nanostructures grown on three-dimension graphene foams for supercapacitors electrodes, Appl. Surf. Sci. 305 (2014) 433 – 438.

[15] M. Zhang, M. Jia, Y. Jin, X. Shi, Synthesis and electrochemical performance of CoO/graphene nanocomposite as anode for lithium ion batteries, Appl. Surf. Sci. 263 (2012) 573 – 578.

[16] X.-l. Huang, R.-z. Wang, D. Xu, Z.-l. Wang, H.-g. Wang, J.-j. Xu, Z. Wu, Q.-c. Liu, Y. Zhang, X.-b. Zhang, Homogeneous CoO on Graphene for Binder-Free and Ultralong-Life Lithium Ion Batteries, Adv. Funct. Mater. 23 (2013) 4345–4353.

[17] J. Wu, D. Carlton, J. S. Park, Y. Meng, E. Arenholz, A. Doran, a. T. Young, A. Scholl, C. Hwang, H. W. Zhao, J. Bokor, Z. Q. Qiu, Direct observation of imprinted antiferromagnetic vortex states in CoO/Fe/Ag(001) discs, Nat. Phys. 7 (2011) 303–306.

[18] M. Finazzi, L. Du, F. Ciccacci, Magnetic properties of interfaces and multilayers based on thin antiferromagnetic oxide films, Surf. Sci. Rep. 64 (2009) 139 – 167.

[19] L. Duò, M. Finazzi, F. Ciccacci (Eds.), Magnetic Properties of Antiferromagnetic Oxide Materials, WILEY-VCH Verlag GmbH & Co. KGaA, Weinheim, 2010.

[20] F. Mittendorfer, M. Weinert, R. Podloucky, J. Redinger, Strain and Structure Driven Complex Magnetic Ordering of a CoO Overlayer on Ir(100), Phys. Rev. Lett. 109 (2012) 015501.

[21] C. Ge, X. Wan, E. Pellegrin, Z. Hu, S. Manuel Valvidares, A. Barla, W.-I. Liang, Y.-H. Chu, W. Zou, Y. Du, Direct observation of rotatable uncompensated spins in the exchange bias system Co/CoO-MgO, Nanoscale 5 (2013) 10236–10241.

[22] A. D. Lamirand, M. M. Soares, A. Y. Ramos, H. C. N. Tolentino, M. De Santis, J. C. Cezar, A. de Siervo, M. Jamet, Robust perpendicular exchange coupling in an ultrathin CoO/PtFe double layer: Strain and spin orientation, Phys. Rev. B 88 (2013) 140401.

[23] P. Kuświk, P. L. Gastelois, M. M. Soares, H. C. N. Tolentino, M. De Santis, A. Y. Ramos, A. D. Lamirand, M. Przybylski, J. Kirschner, Effect of CoO/Ni orthogonal exchange coupling on perpendicular anisotropy of Ni films on Pd(001), Phys. Rev. B 91 (2015) 134413.

[24] S.-C. Chang, J.-S. Tsay, C.-H.-T. Chang, Y.-D. Yao, Pinning of magnetic moments at the interfacial region of ultrathin CoO/Co bilayers grown on Ge(1 0 0), Appl. Surf. Sci. 354, Part A (2015) 95 – 99. 7th Vacuum and Surface Sciences Conference of Asia and Australia (VASSCAA-7).

[25] J. Nogués, I. K. Schuller, Exchange bias, J. Magn. Magn. Mater. 192 (1999) 203.

[26] J. Nogués, J. Sort, V. Langlais, V. Skumryev, S. Suriñach, J. Muñoz, M. Baró, Exchange bias in nanostructures, Phys. Rep. 422 (2005) 65 – 117.

[27] T. J. Regan, H. Ohldag, C. Stamm, F. Nolting, J. Lüning, J. Stöhr, R. L. White, Chemical effects at metaloxide interfaces studied by x-ray-absorption spectroscopy, Phys. Rev. B 64 (1998) 214422.

[28] A. Brambilla and P. Sessi and M. Cantoni and L. Duò and M. Finazzi and F. Ciccacci, Epitaxial growth and characterization of CoO/Fe(001) thin film layered structures, Thin Solid Films 516 (2008) 7519 – 7524.

[29] E. Młyńczak, J. Gurgul, J. Przewoźnik, D. Wilgocka-Ślęzak, K. Freindl, N. Spiridis, J. Korecki, Effect of interfacial iron oxidation on the exchange bias in CoO/Fe bilayers, Appl. Surf. Sci. 304 (2014) 86 – 90. Selected Papers from the 6th International Workshop on Surface Physics Functional Materials.

[30] A. Brambilla, A. Picone, M. Finazzi, L. Duò, F. Ciccacci, Scanning tunneling microscopy investigation of CoO/Fe(001) and Fe/CoO/Fe(001) layered structures, Surf. Sci. 605 (2011) 95 – 100.

[31] F. Donati, P. Sessi, S. Achilli, A. Li Bassi, M. Passoni, C. S. Casari, C. E. Bottani, A. Brambilla, A. Picone, M. Finazzi, L. Duò, M. I. Trioni, F. Ciccacci, Scanning tunneling spectroscopy of the Fe(001)-$p$(1 x 1)O surface, Phys. Rev. B 79 (2009) 195430.

[32] A. Picone, A. Brambilla, A. Calloni, L. Duò, M. Finazzi, F. Ciccacci, Oxygen-induced effects on the morphology of the Fe(001) surface in out-of-equilibrium conditions, Phys. Rev. B 83 (2011) 235402.

[33] S. K. Kim, C. Petersen, F. Jona, P. M. Marcus, Ultrathin films of cobalt on Fe001 and the effect of oxygen, Phys. Rev. B 54 (1996) 2184–2190.

[34] A. Picone, M. Riva, G. Fratesi, A. Brambilla, G. Bussetti, M. Finazzi, L. Duò, F. Ciccacci, Enhanced Atom Mobility on the Surface of a Metastable Film, Phys. Rev. Lett. 113 (2014) 046102.

[35] L. Duò, R. Bertacco, G. Isella, F. Ciccacci, M. Richter, Electronic and magnetic properties of the Co/Fe(001) interface and the role of oxygen, Phys. Rev. B 61 (2000) 15294–15301.

[36] M. Riva, A. Picone, D. Giannotti, A. Brambilla, G. Fratesi, G. Bussetti, L. Duò, F. Ciccacci, M. Finazzi, Oxidation effects on ultrathin Ni and Cr films grown on Fe(001): A combined scanning tunneling microscopy and Auger electron spectroscopy study, Phys. Rev. B 92 (2015) 115434.

[37] A. Calloni, A. Picone, A. Brambilla, M. Finazzi, L. Duò, F. Ciccacci, Effects of temperature on the oxygen aided Cr growth on Fe(001), Surf. Sci. 605 (2011) 2092 – 2096.

[38] A. Picone, G. Bussetti, M. Riva, A. Calloni, A. Brambilla, L. Duò, F. Ciccacci, M. Finazzi, Oxygen-assisted Ni growth on Fe(001): Observation of an "anti-surfactant" effect, Phys. Rev. B 86 (2012) 075465.

[39] A. Picone, G. Fratesi, M. Riva, G. Bussetti, A. Calloni, A. Brambilla, M. I. Trioni, L. Duò, F. Ciccacci, M. Finazzi, Self-organized chromium oxide monolayers on Fe(001), Phys. Rev. B 87 (2013) 085403.

[40] A. Tange, C. Gao, W. Wulfhekel, J. Kirschner, Growth and magnetic order of Mn films on Fe(001)-$p(1\times1)$ studied by spin-polarized scanning tunneling microscopy, Phys. Rev. B 81 (2010) 220404.

[41] M. Riva, A. Picone, G. Bussetti, A. Brambilla, A. Calloni, G. Berti, L. Duò, F. Ciccacci, M. Finazzi, Oxidation effects on ultrathin Ni and Cr films grown on Fe(001): A combined scanning tunneling microscopy and Auger electron spectroscopy study, Surf. Sci. 621 (2014) 55 – 63.

[42] G. Castro, J. Küppers, Interaction of oxygen with hcp (0001) recrystallized cobalt surfaces, Surf. Sci. 123 (1982) 456 – 470.

[43] G. C. Gazzadi, A. Borghi, A. di Bona, S. Valeri, Epitaxial growth of CoO on the (001) surface of bct cobalt, Surf. Rev. Lett. 402-404 (1998) 632–635.

[44] D. R. Lide (Ed.), CRC Handbook of Chemistry and Physics, Internet Version, CRC Press, Boca Raton, FL (USA), 2005.

[45] A. Calloni, G. Berti, A. Brambilla, M. Riva, A. Picone, G. Bussetti, M. Finazzi, F. Ciccacci, L. Duò, Electron spectroscopy investigation of the oxidation of ultra-thin films of Ni and Cr on Fe(0 0 1), J. Phys.: Condens. Matter 26 (2014) 445001.

[46] S. Tanuma, C. J. Powell, D. R. Penn, Calculations of electron inelastic mean free paths. V. Data for 14 organic compounds over the 50-2000 eV range, Surf. Interface Anal. 21 (1994) 165–176.

[47] A. Borghi, A. di Bona, D. Bisero, S. Valeri, Structural and compositional stability of Co oxide grown on (001) bct Co, Appl. Surf. Sci. 150 (1999) 13 – 18.

[48] M. C. Biesinger, B. P. Payne, A. P. Grosvenor, L. W. Lau, A. R. Gerson, R. S. Smart, Resolving surface chemical states in XPS analysis of first row transition metals, oxides and hydroxides: Cr, Mn, Fe, Co and Ni, Appl. Surf. Sci. 257 (2011) 2717 – 2730.

[49] K. G. Nath, Y. Haruyama, T. Kinoshita, Observation of the satellite signal in Co $2p$ photoemission spectra: Evidence of a localized electronic structure in thin films, Phys. Rev. B 64 (2001) 245417.

[50] S. Benedetti, H. M. Benia, N. Nilius, S. Valeri, H. J. Freund, Morphology and optical properties of MgO thin films on Mo(0 0 1), Chem. Phys. Lett. 430 (2006) 330–335.

[51] S. Benedetti, P. Torelli, S. Valeri, H. M. Benia, N. Nilius, G. Renaud, Structure and morphology of thin MgO films on Mo(001), Phys. Rev. B 78 (2008) 1–8.

[52] S. Stuckenholz, C. Büchner, M. Heyde, H.-J. Freund, MgO on Mo(001): Local Work Function Measurements above Pristine Terrace and Line Defect Sites, J. Phys. Chem. C 119 (2015) 12283–12290.

[53] M. Dynna, J. L. Vassent, A. Marty, B. Gilles, A low-energy electron diffraction investigation of the surface deformation induced by misfit dislocations in thin MgO films grown on Fe(001), J. Appl. Phys. 80 (1996) 2650.

[54] J. Wollschläger, D. Erdös, H. Goldbach, Growth of NiO and MgO films on Ag (100), Thin Solid Films 400 (2001) 1–8.

[55] T. Michely, J. Krug, Islands, Mounds and Atoms, volume 42 of *Springer Series in Surface Sciences*, Springer-Verlag Berlin Heidelberg, first edition, 2004.

[56] J. A. Stroscio, D. Pierce, M. D. Stiles, A. Zangwill, Coarsening of unstable surface features during Fe(001) homoepitaxy, Phys. Rev. Lett. 75 (1995) 4246.

[57] I. Horcas, R. Fernández, J. M. Gómez-Rodríguez, J. Colchero, J. Gómez-Herrero, A. M. Baro, WSXM: A software for scanning probe microscopy and a tool for nanotechnology, Rev. Sci. Instrum. 78 (2007) 013705.

[58] M. Kalff, P. Šmilauer, G. Comsa, T. Michely, No coarsening in Pt(111) homoepitaxy, Surf. Sci. 426 (1999) L447 – L453.